Inorganica Chimica Acta, 8 (1974) 323–343

Invited Review

The Physical Properties of Some Transition Metal Compounds of the ABX_3 Type

J.F. ACKERMAN, G.M. COLE and S.L. HOLT
Department of Chemistry, University of Wyoming, Laramie, Wyoming 82070, U.S.A.
Received October 12, 1973

Contents

Summary

Although cooperative phenomena in the solid state are most commonly two dimensional, [2], or three dimensional, [3] in nature, it is from one dimensional, [1], systems that the most information can be garnered. The physical properties of a class of compounds of the formulation ABX_3 which display [1] structures are reviewed.

1. Introduction

Recently, considerable effort has been expended by theoreticians and experimentalists in order to understand the nature of antiferromagnetically coupled systems. Of particular interest has been identification of spin waves (magnons) at temperatures above T_n and the relationship of these spin waves to anomalous effects in the optical spectra of solid insulators.[1] While the presence of magnons is common to antiferromagnetically (and ferromagnetically) coupled systems, no matter what their dimensionality, it is in the one dimensional [1], case where the theoretical problem has its simplest

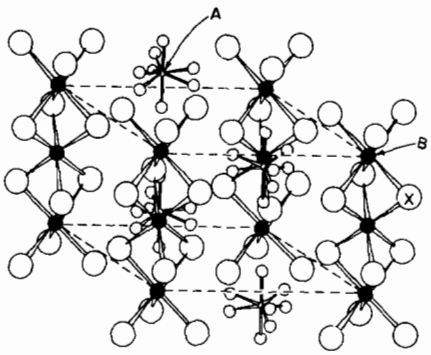

Figure 1A. Unit cell for a typical ABX_3 linear chain compound. Here $A=(CH_3)_4N^+$. Adopted from Ref. 4.

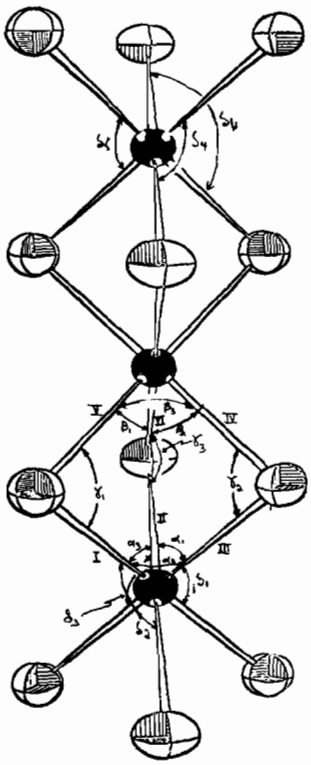

Figure 1B. A portion of the linear chain of a typical ABX_3 compound showing angles and bond lengths referred to in Table II. Adopted from Ref. 20.

TABLE I. Structural data for ABX_3 Compounds.

Compound	Space Group	Lattice Constants (Å)	Structural Type	B–B (Å)	B–X (Å)	B–X–B° [a]	X–B–X° [a]	B–B′ (Adjacent Chains) (Å)
$CsCuCl_3$[2]	$P6_122$	a = 7.2157(5) c = 18.1777(10)	Linear chain of face sharing distorted $[CuCl_6]^{4-}$ octahedra. Forms [1] network.	3.0621(10)	II, VI = 2.355(4) III, V = 2.776(6) I, IV = 2.281(6)	γ_2 = 81.12 γ_1, γ_3 = 73.80	α_1 = 89.30, α_3 = 90.52 α_2 = 78.38, δ_1 = 95.44 δ_4 = 90.32, δ_5 = 95.52	7.2157
$CsCuBr_3$[3]	$C222_1$	a = 12.776(2) b = 7.666(2) c = 12.653(4)	Face sharing $[Cu_2Br_9]^{5-}$ dimers, which in turn share corners with six other dimers to form [3] network.	3.257(5) within dimeric unit	I, V = 2.482(4) II, VI = 2.868(4) III, IV = 2.460(4) *trans* I = 2.522(3) *trans* II = 2.959(5) *trans* III = 2.541(5)	γ_1 = 82.02(16) γ_2 = 74.94(12) γ_3 = 74.94(12) Bridging from dimer to dimer = 167.60(18)	α_3 = 79.86(10) *(interior)* α_1 = 87.38(11) *(interior)* β_1 = 91.17(12) *(exo)* β_2 = 89.97(8) *(exo)* δ_1 = 90.32(13) *(interior–exo)*	5.029(5) between Cu in parent dimer and Cu in dimer bound through terminal bromine
$(CH_3)_4NNiCl_3$[4]	$P6_3$	a = 9.019(1) c = 6.109(1)	Linear chain of face sharing $[NiCl_6]^{4-}$ octahedra. Ni^{2+} site symmetry is C_{3d}.	3.577	2.408(1)	78.74(4)	84.05(4)	9.019(1)
$(CH_3)_4NNiBr_3$[5]	$P6_3$	a = 9.35(2) c = 6.35(1)	Linear chain of face sharing $[NiBr_6]^{4-}$ octahedra Ni^{2+} site symmetry is C_{3v}.	3.17(1)	I–III = 2.67(1) IV–VI = 2.45(1)	γ_1–γ_3 = 76.45(19)	α_1–α_3 = 80.86(26) β_1–β_3 = 90.45(28) δ_1–δ_3 = 94.17(27)	9.35(2)
$CsNiCl_3$[6]	$P6_3/mmc$	a = 7.18 c = 5.93	Linear chain of face sharing $[NiCl_6]^{4-}$ octahedra. Ni^{2+} site symmetry is D_{3d}.	2.97				7.18

TABLE I. (Cont.)

Compound	Space Group	Lattice Constants (Å)	Structural Type	B–B (Å)	B–X (Å)	B–X–B° [a]	X–B–X° [a]	B–B' (Adjacent Chains) (Å)
$CsNiBr_3$[5]	$P6_3/mmc$	a = 7.50(2) c = 6.24(1)	Isomorphous and isostructural with $CsNiCl_3$.	3.12				7.50
$CsNiI_3$[7]	$P6_3/mmc$	a = 8.00 c = 6.76	Isomorphous and isostructural with $CsNiCl_3$					8.00
$RbNiCl_3$[8]	$P6_3/mmc$	a = 6.955(1) c = 5.906(1)	Isomorphous and isostructural with $CsNiCl_3$.	2.9530(5)	I–VI = 2.396(3)		δ_1–δ_3 = 94.01(8) α_1–α_3, β_1–β_3 = 85.99(8)	6.955(1)
$RbNiBr_3$[8]	$P6_3/mmc$	a = 7.268(8) c = 6.208(8)	Isomorphous and isostructural with $CsNiCl_3$.	3.104(4)	I–VI = 3.51			7.268(8)
$CH_3NH_3NiCl_3$[9]	Cmcm	a = 6.94 b = 14.94 c = 5.95	Linear chain of face sharing $[NiCl_6]^{4-}$ octahedra. Ni^{2+} site symmetry is C_{2v}.	3.12	III = 2.351 V = 2.405	γ_1 = 76.4 γ_2 = 78.5	β_1 = 86.2 β_2 = 81.6 δ_1 = 93.7	6.94(2)
$TlNiCl_3$[10]	$P6_3mc$	a = 6.863 c = 5.881	Linear chain of face sharing $[NiCl_6]^{4-}$ octahedra.	2.94 [b]	I–VI = 2.47	γ_1–γ_3 = 73.18 [b]	α_1–α_3 = 88.17	6.863
$CsCoCl_3$[11]	$P6_3/mmc$	a = 7.2019(4) c = 6.0315(5)	Isomorphous and isostructural with $CsNiCl_3$.	3.0158(3)	I–VI = 2.447(3)		$\delta_1, \delta_2, \delta_3$ = 93.99(4) $\alpha_1, \alpha_2, \alpha_3, \beta_1, \beta_2, \beta_3$ = 86.01	7.2019(4)
$RbCoCl_3$[12]	$P6_3/mmc$	a = 6.999(1) c = 5.996(1)	Isomorphous and isostructural with $CsNiCl_3$.	2.998(1)	I–VI = 2.46(2)		δ_1–δ_3 = 93.3(5) α_1–α_3, β_1–β_3 = 86.7(5)	6.999(1)

TABLE I. (Cont.)

Compound	Space Group	Lattice Constants (Å)	Structural Type	B–B (Å)	B–X (Å)	B–X–B° [a]	X–B–X° [a]	B–B′ (Adjacent Chains) (Å)
NH_4CoCl_3[13]	$P6_3mc$		Isomorphous and isostructural with NH_4FeCl_3.					
$TlCoCl_3$[10]	$P6_3mc$	a = 6.907 c = 5.981	Isomorphous and isostructural with $TlNiCl_3$.	2.9905[b]	I–VI = 2.49[b]	γ_1–γ_3 = 73.7560[b]	α_1–α_3, β_1–β_3 = 87.69[b]	6.907
$CsFeCl_3$[14]	$P6_3/mmc$	a = 7.238 c = 6.05	Isomorphous and isostructural with $CsNiCl_3$.	3.03[b]	I–VI = 2.49[b]	γ_1–γ_3 = 74.75	α_1–α_3, β_1–β_3 = 113.41[b]	7.238
$RbFeCl_3$[14]	$P6_3/mmc$	a = 7.060(5) c = 6.020(8)	Isomorphous and isostructural with $CsNiCl_3$.	3.53				7.060(5)
NH_4FeCl_3[13]	$P6_3mc$	a = 7.019(6) c = 6.058(6)	Isomorphous and isostructural with NH_4CoCl_3.	3.03[b]	I–VI = 2.53[b]	γ_1–γ_3 = 73.57[b]	α_1–α_3, β_1–β_3 = 87.83[b]	7.019(6)
$TlFeCl_3$[10]	$P6_3mc$	a = 6.976 c = 6.008	Isomorphous and isostructural with $TlNiCl_3$.	3.00[b]	I–VI = 2.51	γ_1–γ_3 = 73.46[b]	α_1–α_3, β_1–β_3 = 87.91[b]	6.976
$(CH_3)_4NMnCl_3$[15]	$P6_3m$(300° K)	a = 9.1510(9) c = 6.4940(9)	Linear chain of face sharing $[MnCl_6]^{4-}$ octahedra. Mn lies on site of D_{3d} symmetry.	3.25[b]	I–VI = 2.56[b]	γ_1–γ_3 = 78.69[b]	α_1–α_3, β_1–β_3 = 84.09[b]	9.15
$(CH_3)_4NMnCl_3$[16]	$P2_1/m$(128° K)	a = 9.27 b = 6.69 c = 8.79; β = 118.6°	As above with apparently no large distortions induced in chain.	4.63	I–VI = 2.560(2)			9.1510

TABLE I. (Cont.)

Compound	Space Group	Lattice Constants (Å)	Structural Type	B–B (Å)	B–X (Å)	B–X–B° [a]	X–B–X° [a]	B–B′ (Adjacent Chains) (Å)
$CsMnCl_3$[17]	$R\bar{3}m$	a = 7.290(5) c = 27.317(4)	Linear chains of face sharing $[MnCl_6]^{4-}$ octahedral trimers. Trimers share terminal corners in such a way that the trimers spiral around the trigonal axis. Central $Mn^{2+} = D_{3d}$; terminal $Mn^{2+} = C_{3v}$.		I–III = 2.551 IV–VI = 2.545 *trans* I–III = 2.514		$\alpha_3 = 84.98$ $\beta_1 = 85.50$ *(interior)* $\beta_1 = 92.92$ *(exo)* $\delta_1 = 94.50$ *(interior)* $\delta_1 = 90.92$ *(exo)*	5.028
$CsMnBr_3$[18]	$P6_3/mmc$	a = 7.609(15) c = 6.52(5)	Isomorphous and isostructural with $CsNiCl_3$.	3.26 [b]	I–VI = 2.683(6) [b]	γ_1–γ_3 = 74.82	α_1–α_3, β_1–β_3 = 113.4 [b]	7.609(15)
$(CH_3)_4NCrCl_3$[19]		a = 9.05 c = 6.55		3.27				9.05
$(CH_3)_4NCrBr_3$[19]		a = 9.33 c = 6.74		3.37				9.33
$CsCrCl_3$[20]	$P6_3mc$	a = 7.256(3) c = 6.224(3)	Linear chain of face sharing octahedra, similar to $CsNiCl_3$. Site symmetry of Cr^{2+} is D_3.	3.112(3)	I–III = 2.618	γ_1–γ_3 = 76.20	α_1–α_3 = 81.66 β_1–β_3 = 90.05 γ_1–γ_3 = 94.01	7.256
$CsCrI_3$[17]	$P6_3/mmc$	a = 8.12(2) c = 6.85(2)	Isomorphous and isostructural with $CsNiCl_3$.	3.42				8.12

TABLE I. (Cont.)

Compound	Space Group	Lattic Constants (Å)	Structural Type	B–B (Å)	B–X (Å)	B–X–B° [a]	X–B–X° [a]	B–B′ (Adjacent Chains) (Å)
$RbCrCl_3$[21]		a = 7.03 c = 6.08	Lower symmetry than $CsCrCl_3$.	3.04				7.03
$(CH_3)_4NVCl_3$[22]	$P6_3mc$	a = 9.146 c = 6.227	Isomorphous and isostructural with $(CH_3)_4NNiCl_3$.	3.11				9.146
$CsVCl_3$[22]	(Hexagonal)	a = 7.23 c = 6.03		3.01				7.23
$RbVCl_3$[23]		a = 7.04(1) c = 6.00(1)	Isomorphous and isostructural with $CsNiCl_3$.	3.00				7.04
$CsVI_3$[17]	$P6_3/mmc$	a = 8.21(2) c = 6.81(2)		3.41				8.21

[a] Refer to Figure 1B for correlation between Roman numerals, Greek symbols and corresponding bond lengths and angles.
[b] Calculated from data in parent reference.

TABLE II. Magnetic Data for ABX_3 compounds.

Compound	Direction of Field	μ_{eff} (μ_B)	g-factor		χ_m ($\cdot 10^3$ emu)	T_m (° K)	Θ_p(° K)	T_N(° K)	χ ($\cdot 10^3$ emu) (0° K)	J/k(° K)	
			from χ	from ESR						from T_m	from χ_m
$CsCuCl_3$[25]	powder		2.207				−3.50	≈10	≈19		
$CsCuCl_3$[26]	//	1.89	2.19		18	7.7	3		17.2	−7.0	−7.3
	⊥	1.89	2.19		21	9.0	6		20.1	−6.0	−6.3
$CsCuCl_3$[27]	//							10		−7.6	
	⊥									−6.5	
$CsCuBr_3$[3]	powder	0.11(296° K)									
$(CH_3)_4NNiCl_3$[28]	powder	3.19[a]	2.262		3.338	1.6	0			1.9	
$N–C_3H_7NH_3NiCl_3$[29]	powder	3.32					−40				
$C_5H_5NHNiCl_3$[29]	powder	3.39					−36				
$C_5H_5NHNiBr_3$[29]	powder	3.40					−32				
$CsNiCl_3$[29]	powder	3.37					−76				
$CsNiCl_3$[26]	//	3.41(polycrystal)	2.41(polycrystal)	2.24(77° K)	12.1	35	−69(polycrystal)	4.5	3.5	−11.0	−12.1
	⊥			2.28(77° K)	12.2	35			7.3		
$CsNiCl_3$[30]											−13
$CsNiCl_3$[31]	powder			2.25	12.73	30					−14.2
$CsNiBr_3$[29]	powder	3.42					−101				
$RbNiCl_3$[29]	powder	3.47					−112				
$RbNiCl_3$[26]	//	3.34(polycrystal)	2.36(polycrystal)	2.21(77° K)	8.93	45	−100(polycrystal)	11	3.8		
	⊥			2.23(77° K)	8.75	45			7.0	−14.1	−16.1
$RbNiCl_3$[30]											−17
$RbNiBr_3$[29]	powder	3.51					−156				
$CH_3NH_3NiCl_3$[29]	powder	3.47					−60				
$CsCoCl_3$[30]	powder	4.77(296.5)									
$CsCoCl_3$[26]	//	6.14	7.4 1% Co^{2+}	7.32(2.4° K)	21.5	85	−90		5.8	−85	−86.1
	⊥	5.54	4.3 in $CsMgCl_3$		18.5	17	−176		18.1	−17(from $\alpha_{//}^2/\alpha_{\perp}^2 = 5$)	
$CsCoCl_3$[30]											≈−115
$CsFeCl_3$[33]	(powder) //	5.76(<90° K)	4.6				−1(<90° K)	~10			−7
	⊥		4.2								−0.5
$RbFeCl_3$[26]	//	6.70(<106° K)	4.74		97.7	12.6	−50(<105° K)		39		−11.5
	⊥	6.35(<85° K)	4.49		492	0	−3(<85° K)		492		−3.8
$RbFeCl_3$[33]	(powder) //		4.6				−3(<80° K)				−5.8
	⊥	5.95(<80° K)	4.25								−1.6

TABLE II (Cont.)

Compound	Direction of Field	μ_{eff} (μ_B)	g-factor		χ_m ($\cdot 10^3$ emu)	T_m (° K)	Θ_p(° K)	T_N(° K)	χ ($\cdot 10^3$ emu) (0° K)	J/k(° K)	
			from χ	from ESR						from T_m	from χ_m
NH_4FeCl_3[33]	(powder) //		4.15				−2.5(<80° K)				−8
	⊥	5.79(<80° K)	4.5								−1.5
$TlFeCl_3$[33]	(powder) //		4.6								−8
	⊥	5.90(<80° K)	4.2				−5.5(<80° K)				−2.7
$(CH_3)_4NMnCl_3$[24]	//				2.4	55					
	⊥				2.3	55		0.84			−6.3
$CsMnCl_3$[34]		6.13					−145				
$CsMnCl_3$[35]								69 ± 3			
$CsMnCl_3$[36]		5.5 ± 0.5						67 ± 2			
$RbMnCl_3$[35]								86 ± 6			
$RbMnCl_3$[37]								≈88			
$RbMnCl_3$[38]		5.3(>250° K)						94 ± 2			
$TlMnCl_3$[39]		4.7 ± 0.2						118 ± 2			
$CsCrCl_3$[40]		3.40						≈108(T_c)			
$CsCrCl_3$[41]		3.31									−35
$(CH_3)_4NVCl_3$[42]		2.13(289° K)			2.7	196					
$CsVCl_3$[42]		1.68(289° K)									
$RbVCl_3$[23]		1.85(300° K)			≈1.4	340	−136	350			−151

[a] Calculated from $\mu_{eff} = 2.84[\chi_M(T-\Theta)]^{1/2}$

proportions. Experimentally, however, one is faced with the difficult task of producing a truly [1] system. As a class of compounds this is most nearly achieved in certain materials of the ABX_3 type. For compounds where A = Rb^+, Cs^+, Tl^+ or $(CH_3)_4N^+$; B = first row transition metal ion; X = Cl^-, Br^- or I^- and for $CH_3NH_3NiCl_3$, NH_4CoCl_3 and NH_4FeCl_3; structures similar to the one in Figure 1 have been shown to exist[2–23], Table I. Here we have continous chains of face sharing BX_6^{4-} octahedra separated by the A cation. The interchain separation is sufficiently large, where A = $(CH_3)_4N^+$, to produce, in $(CH_3)_4NMnCl_3$, [1] magnetic behavior to temperatures as low as 0.84° K[24]. In other ABX_3 systems, where A = Rb^+, Cs^+, Tl^+, or NH_4^+, [3] ordering occurs at much higher temperatures, due to decreased interchain separation[23,25–42], Table II. Clearly then, studies of the physical properties of compounds of the ABX_3 formulation which possess the above structural type provide not only an opportunity to study [1] cooperative effects but to ascertain the effects of interchain vs intrachain coupling.

2. Theoretical Considerations

A. Magnetism in One Dimension

As a basis for a description of deviations from paramagnetic behavior we shall construct our ground state wave functions from Pauli antisymmetrized orbitals. In particular if one uses a 2 atom/2 spin system one arrives at:

$$\Psi = \begin{vmatrix} \Phi_1(1)\,\Phi_2(1) \\ \Phi_1(2)\,\Phi_2(2) \end{vmatrix} \Phi_{spin} = [\Phi_1(1)\,\Phi_2(2) - \Phi_1(2)\,\Phi_2(1)]\Phi_{spin} \quad (1)$$

Matrix elements of this wavefunction with the Coulomb potential e^2/R produce terms such as $[\Phi_1(1)\,\Phi_2(2)\,|e^2/R_{12}|\,\Phi_1(2)\,\Phi_2(1)]\alpha\beta = J\alpha\beta = JS_i \cdot S_j$. This is a ground state energy term which is due to the exchange of the electrons on two different atoms and results in the polarization of the electron spins. When treating a real compound it is necessary to sum the exchange interactions, $JS_i \cdot S_i$ over all spins in the system and their nearest neighbors. In a linear chain this means $JS_iS_j \rightarrow 2\sum_{i=1}^{n} S_{i+1}$. Taking account of an external magnetic field and summing over all atoms provides an additional term $g\beta\sum_{i=1}^{n} H \cdot S_i$. Therefor the total Hamiltonian is of the form

$$H = -2J\sum_{i=1} \{S^z_i S^z_{i+1} + \gamma\,(S^x_i S^x_{i+1} + S^y_i S^y_{i+1})\} - g\beta\sum_{i=1}^{n} H \cdot S_i \quad (2)$$

Here for $-/J/$ we have an antiferromagnetic interaction while $+/J/$ yields a ferromagnetic interaction, i.e.

$-/J/$ ↑↓↑↓
$+/J/$ ↑↑↑↑

There are two limits to the Hamiltonian [Eq. (2)] which need concern us: $\gamma = 1$ and $\gamma = 0$. Where $\gamma = 1$ we have the Heisenberg limit and the interaction is totally isotropic. For $\gamma = 0$ the Ising Model, the interaction is anisotropic. As would be expected neither of these extremes is entirely suitable for the systems to be discussed later. Bonner and Fisher[43] have treated the intermediate, $0<\gamma<1$, case, however, and have shown that the susceptibility parallel to the chain approaches 0 as $T \rightarrow 0$ while the perpendicular susceptibility remains finite as $T \rightarrow 0$ (zero-point deviation). Consequently compounds with even a small anisotropic component of energy will show a marked anisotropic susceptibility as $T \rightarrow 0$. Typical of the result one gets for magnetic susceptibility (χ) when applying the Bonner and Fisher model are the expressions derived by Gerstein *et al.*[28], where g = electronic g-factor and μ_B = Bohr Magneton:

$$\chi_{//} = \frac{N_{g//}{}^2\mu_B{}^2}{kT} \quad \frac{1}{1 + e^{-J/kT}\cosh(J\gamma/kT)}, \quad (3)$$

$$\chi_{\perp} = \frac{N_g{}^2\mu_B{}^2}{J\,(\gamma-1)} \quad \frac{e^{J\gamma/kT} - e^{J/kT}}{e^{J/kT} + \cosh(J\gamma/kT)}, \quad (4)$$

to explain the magnetic behavior of $(CH_3)_2NH_2CuCl_3$. While the above models help us to explain *ex post facto* the behavior of materials some simple qualitative arguments can help predict, in certain cases, whether a compound will be ferro- or anti-ferromagnetic.

Kanamori[44] has discussed the relation between the symmetry of electron orbitals and superexchange interaction, based upon proposals of Anderson[45], Slater[46], and Goodenough[47]. Table III reproduces a series of predictions by Kanamori for the cases of 90° (intrachain) and 180° (interchain) superexchange. These results are obtained, based upon a relatively simple model and should be used as a general guide only. Referring to Figure 2 we assume that the principal covalent bonding occurs *via* the d_z^2 orbital of cation 1 overlapping the pσ orbital of a bridging anion. If we

TABLE III. Results of 90° and 180° Magnetic Interaction Between High Spin Cations in Octahedral Sites.

Number of 3d electrons of interacting cations	Resultant 90° exchange	Resultant 180° exchange
d^1–d^1	ferro	
d^2–d^2	ferro	
d^3–d^3	ferro	antiferro
d^4–d^4	uncertain	
d^5–d^5	uncertain	antiferro
d^6–d^6	uncertain	antiferro
d^7–d^7	uncertain	antiferro
d^8–d^8	ferro	antiferro
d^9–d^9	ferro	

neglect the possibility of the t_{2g} set of orbitals π-bonding with the $p\sigma$ orbital of the anion and the additional possibility of any exchange through metal–metal overlap we can see that the magnetic behavior will be dominated by the σ interaction. Further we can consider the σ(p–d) interaction to dominate the σ(s–d) interaction. The mechanism by which the super-exchange process occurs then involves a transfer of an electron from the $p\sigma$ orbital of the anion to the d_z2 orbital of cation 1 followed by the coupling of the now 'unpaired' spin on the anion with the electrons in the d-orbitals of cation 2 *via* exchange interaction. If the exchange is between the $p\sigma$ orbital and the orthogonal d_z2 orbital and the non-orthogonal t'_{2g} set the exchange will be antiferromagnetic[48]. Applying these conditions to the case of coupled Cr^{3+} ions provides us with an example of how this model can be used in certain cases to predict magnetic behavior.

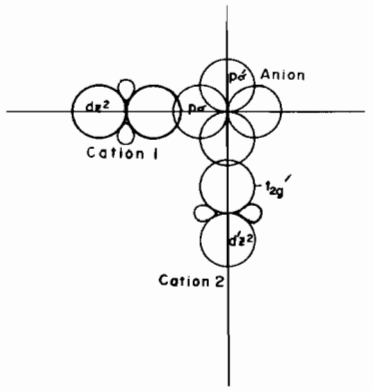

Figure 2. 90° exchange path between two interacting metal ions.

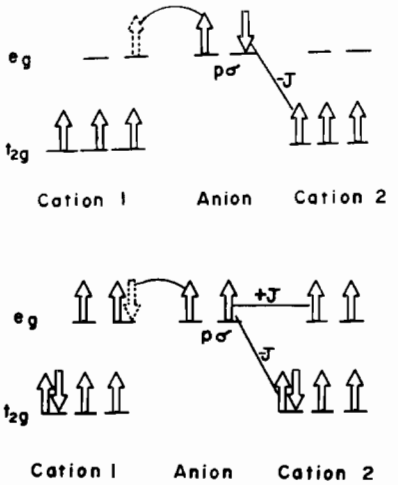

Figure 3. Superexchange Pathway in (a) 90° bonded Cr^{3+}–Cr^{3+}; (b) 90° bonded Fe^{2+}–Fe^{2+}.

Chromium (III) is a d^3 system, consequently the low lying t_g^2 orbitals are half-filled, Figure 3. Upon bonding there is a transfer of a $p\sigma$ electron from the anion to the d_z^2 orbital of cation 1. Because the e_g set is unoccupied the spin alignment of the p_σ–d_{z2} electron is dictated by exchange interaction with the electrons in the nonorthogonal t_g^2 set. This results in a parallel alignment (↑ in Figure 3). The 'unpaired' electron in the $p\sigma$ orbital then will be ↓. Because the e_g set of orbitals are unoccupied the exchange interaction between this electron and electrons in cation 2 is directed toward the nonorthogonal t_g^2 set. This exchange will be antiferromagnetic, giving rise to ferromagnetic Cr^{3+}–Cr^{3+} coupling.

For the case of six d-electrons the situation is somewhat more complex. The Pauli principle requires that the electron donated from the anion pair with the electron which already resides in the d_{z2} orbital. The remaining anion electron can then couple ferromagnetically with the electrons in the e_g orbitals of cation 2 or antiferromagnetically with those in the t_g^2 orbitals. In addition bonding between the $p\sigma$ orbital of the anion and the t'_{2g} orbitals of cation 2 will provide a further complication. Therefore we must regard the situation in this case as uncertain and no prediction can be made. Indeed in ~50% of the cases one must await the experiment before anything may be said about the mechanism, however, from the conceptual standpoint the model is highly useful.

B. Optical Manifestation of Cooperative Effects in Magnetically Concentrated Systems

(i) Single exciton transitions

Crystal field theory has been widely applied to the spectra of transition metal systems. Inherent in the application has been the assumption that the molecular or ionic unit containing the transition metal ion may be treated as an isolated, and sometimes oriented, gas; i.e., interactions between adjacent metal ions may be ignored. This assumption is a perfectly valid one when the transition metal ion under study is embedded in a nonmagnetic host having no optical structure in the region of study. However, simple crystal field theory is inadequate to explain completely all the optical phenomena which occur when the concentration of the active ion is sufficient to allow pairwise interactions to become important. Indeed in a pure crystal in those cases where direct avenues of exchange exist between neighboring transition metal ions, it is unwise even to limit ones frame of reference to so small an aggregate as a pair. Strictly speaking we should consider collective excitations of the whole crystal. These collective excitations are generally referred to as excitons. There are two limiting approximations for excitons: the weak binding or Wannier formalism and the tight binding or Frenkel

approximation.[49] It is the latter formalism which is important to us. In this theory the electrons remain tightly bound to a given ion and an ionic excitation propogates (A Wannier exciton is an electron–hole pair which propogate separately). These excitons are then a linear combination of single-ion excitations.[50] In general we simplify the physical problem by assuming that we may neglect coupling between non-degenerate ionic states which are separated by large energies when compared to interionic coupling, e.g. a separation of a few hundred cm^{-1} is more than adequate. Since it is in the spin-forbidden transitions, i.e. $^{(2S+1)}\Gamma \rightarrow {}^{(2S+1)-2}\Gamma'$, that the major effects of interionic coupling will be seen to manifest themselves, we can simplify our picture by noting that in a unique two sublattic system (i.e. an antiferromagnet) the z component of the spin-angular-momentum will change by 2 upon transfer of an excitation from one sublattice to another.[51] This is a highly forbidden process and leads to the result that for *transfer* of a spin-forbidden excitation an intrasublattice process is greatly favored over an intersublattice process. Because of this the sublattice excitons become eigenstates of the system. This allows us to treat single excitons within the framework of a transition localized on a single ion.[52] In support of this idea are the results of Dietz and Misetich[53] who found that the E1 and E2 excitons in MnF_2 have no measurable dispersion.

(ii) Exciton–exciton transitions

An exciton–exciton (or double exciton) transition involves both sublattices of a two sublattic antiferromagnet. This process is a two-center excitation whereby a photon simultaneously excites ions on opposite sublattices, Figure 4. Therefore, as with the single exciton case we are interested only in the spin-forbidden transitions. Since the z-components of the spin angular momenta of the two coupled ions are in opposition in the ground state as well as in the excited state the total spin of the system is conserved ($\Delta S = 0$) even though both ions have undergone a $\Delta S = 1$ transition. Not surprisingly then we would expect double exciton transitions to be considerably more intense than single exciton transitions. Indeed in MnF_2 the double exciton line, E22, has been found to have nearly three times the oscillator strength of the single exciton line E2[52,54].

(iii) Exciton–magnon transitions

A magnon is little more than a low energy exciton. In an ordered system, be it ferromagnetic or anti-ferromagnetic, a coupled array of spins exists. If a low energy excitation is impinged upon one spin, causing a spin

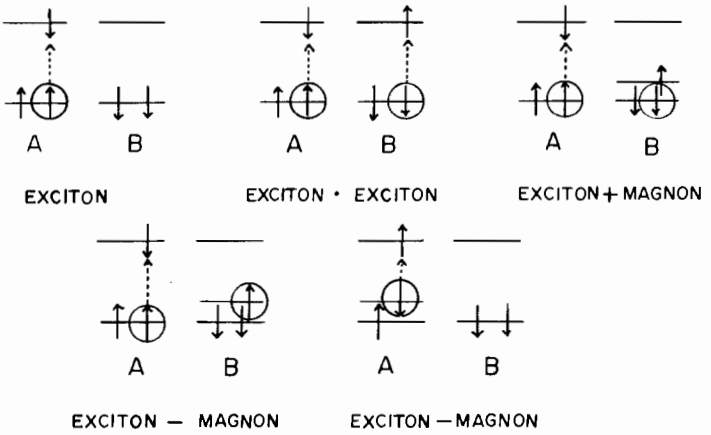

Figure 4. Exciton and exciton magnon processes. A and B refer to opposite sublattices.

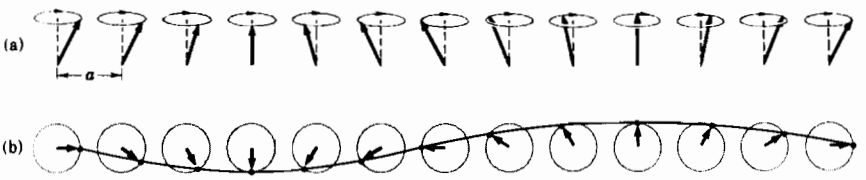

Figure 5. Schematic representation of a spin-wave or magnon. (a) View in the a c–plane. (b) View in the a b–plane. Adopted from Ref. 96.

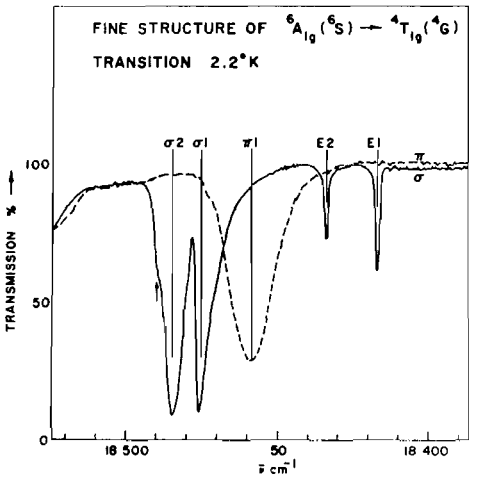

Figure 6. Exciton (E1, E2) and exciton + magnon ($\pi 1, \sigma 1, \sigma 2$) transitions in MnF_2. Adopted from Ref. 52.

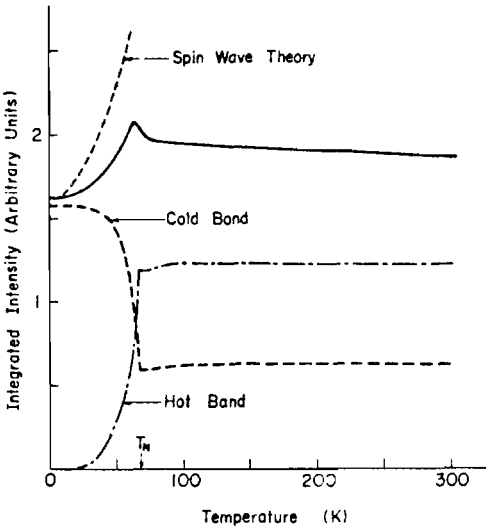

Figure 7. Calculated temperature dependence of magnon side bands in MnF_2. Adopted from Ref. 57.

deviation, this deviation will be transmitted to a coupled next nearest neighbor and so on, down the chain, (see Figure 5). This is called a spin wave or magnon. In the more localized sense we can consider a magnon as a spin deviation i.e. 'localized spin-wave' on an individual ion. It should be clear then that the $\Delta S = 0$ requirement for a transition can be accomplished by the simultaneous creation of an exciton on one sublattice and a magnon on the sublattice of opposite spin, Figure 4. This is called an *exciton + magnon* transition and will occure at higher energies than the pure exciton transition, Figure 6. On the other hand, if a magnon is created on a sublattice we can also obtain a $\Delta S = 0$ transition. Now, however, our ground state for the transition is really the magnon excited state. Therefore our absorption peak will occur at a energy less than that of the pure exciton. This is an *exciton–magnon*.

There is a second way to produce an *exciton–magnon*. This involves annihilating a magnon on sublattice 2 while creating on exciton on sublattice 1. Clearly this process is similar to the earlier *exciton–magnon* process but involves both sublattices as opposed to only one.

(iv) Temperature dependence

For the single exciton transitions one would expect the classical dependence of oscillator strength on temperature: $f(T) = f(0) \coth \frac{h\omega}{2kT}$ where ω is the mean frequency of the odd lattice modes which perturb the inversion symmetry of the metal atom site. This, of course, will not apply to *magnon ± exciton* transitions.

The temperature dependence of exciton/magnon transitions has been treated theoretically for MnO and MnS[55] and for MnF_2 and $RbMnF_3$.[56–59] The calculated

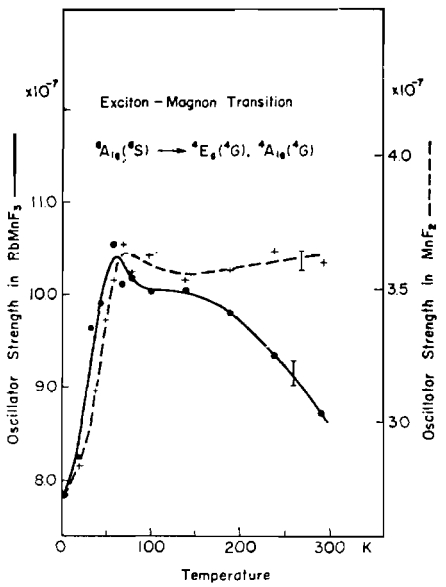

Figure 8. Experimental temperature dependence of oscillator strengths for the exciton–magnon transition $^6A_{1g}(^6S) \rightarrow {}^4E_g(^4G)$, $^4A_{1g}(^4G)$ in MnF_2 and $RbMnF_3$. Adopted from Ref. 59.

temperature variation of magnon side bands in MnF_2 is shown in Figure 7.[57,59] This suggests that the major change in oscillator strength should occur below T_N. The magnitude of that change will depend upon the relative contribution of magnon hot bands *(exciton–magnon)*, magnon cold bands *(exciton + magnon)* and phonon modes. Experimentally it is found that the oscil-

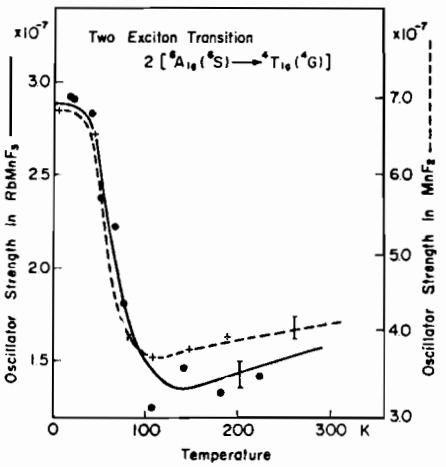

Figure 9. Experimental temperature dependence of oscillator strengths for the double exciton transition $2[^6A_{1g}(^6S)\rightarrow{}^4T_{1g}(^4G)]$ in MnF_2 and $RbMnF_2$. Adopted from Ref. 59.

lator strength of the exciton/magnon transitions may increase or decrease slightly in going from room temperature to T_N but that there is a major decrease in oscillator strength below T_N[59], Figure 8. On the other hand, the double exciton transition $2[^6A_{1g}\rightarrow{}^4T_{1g}]$, in MnF_2 and $RbMnF_3$ shows a marked increase in intensity below T_N, Figure 9.[59]

C. Magnetic Resonance Spectroscopy

At the present time the use of magnetic resonance techniques is a singularly undevloped area as applied to [1] linear chains. The techniques which we shall briefly consider are electron spin resonance (ESR) and nuclear magnetic resonance (NMR).

(i) ESR

There are two magnetically distinct regions of concern: a paramagnetic region above T_N and an ordered region below T_N. Since most of the ESR results reviewed in Section 4 are limited to the paramagnetic region, we shall omit discussion of ESR below T_N[60].

Consider a linear chain of paramagnetic ions in which the ions are isolated from each other. Due, for example, to slight variations in local symmetries, the magnetic field and hence the resonance frequency at each ion will be slightly different. This results in an "inhomogeneously" broadened resonance signal. If we then allow the individual spin magnetic moments to become correlated so that each ion "sees" its neighbors, the local fields will tend to become increasingly homogeneous. The resonance signal will be narrowed roughly in proportion to the strength of the correlation. In most [1] linear chains the coupling mechanism is not a simple exchange interaction arising from direct overlap of metal ion wavefunctions, but rather to one or more superexchange paths arising from paramagnetic spin density transfered from one metal ion through orbitals of the bridging ligands to an adjacent metal. A distinctive feature of [1] linear chains – and one which causes difficulty in interpreting ESR spectra – is the development of short range magnetic order without a definite transition to long range order.

The form of the Hamiltonian is highly dependent on the particular system in question, but, in general, we may write

$$H = \underset{\sim}{D}\sum_i [(S_i^z)^2 + (S_j^z)^2] - 2\underset{\sim}{J}_{//} \sum_{i,j} S_i^z S_j^z - J_\perp \sum_{i,j} S_i^x S_j^y - \underset{\sim}{g}_{//}\mu_B \underset{\sim}{H}^z \sum_i (S_i^z + S_j^z) - {}^1/_2\, g\mu_B H (S_i^x + S_j^y). \quad (5)$$

In the first term of Eq. (5) $\underset{\sim}{D}$ is the zero-field parameter; the second and third terms represent the parallel and perpendicular exchange interactions; and the second line represents the parallel and perpendicular electronic Zeeman interactions.

(ii) NMR

Most NMR investigations of $ABCl_3$ compounds have focused on ^{35}Cl. The spectra can be analyzed to obtain the nuclear quadrupole coupling constants and the parallel and perpendicular magnetic superhyperfine (shf) coupling constants, $\underset{\sim}{A}_{//}$ and $\underset{\sim}{A}_\perp$, respectively. The shf parameters are important in that they may be related to ligand molecular orbital coefficients.

We first define isotropic and anisotropic shf constants as

$$A_s = {}^1/_3(2A_\perp + A_{//}) \quad (6)$$

and

$$A_{\sigma-\pi} = {}^1/_3(A_{//} - A_\perp) \quad (7)$$

respectively. It may be shown[61] that

$$A_s = Z^{-1}\left(\frac{\gamma_s^2}{N}\right) A_{3s} \quad (8)$$

and

$$A_{\sigma-\pi} = Z^{-1}\left(\frac{\lambda_\sigma^2 - \lambda_\pi^2}{N}\right) A_{3p} \quad (9)$$

where $\underset{\sim}{Z}$ is the coordination number of the complex, A_{3s} and A_{3p} are the calculated atomic hyperfine constants respectively, and λ_s, λ_σ and λ_π are molecular orbital coefficients for ligand s, pσ and pπ orbitals, respectively. The covalency parameters are then defined as

$$f_s = 2S\left(\frac{A_s}{A_{3s}}\right), \quad (10)$$

$$f_{\sigma-\pi} = 2S\left(\frac{A_{\sigma-\pi}}{A_{3p}}\right) \quad (11)$$

where S is an overlap integral. The covalency parameters represent the fractional *paramagnetic* spin density of the metal-ion electrons transfered to the ligands.

In a similar manner we may write the fractional transfered *electronic* spin density along the direction of maximum field gradient.[61] As a ratio of the measured quadrupole coupling constant to the atomic coupling constant:

$$f_Q = \left(\frac{(eqQ)}{(eqQ)_{At}}\right) \quad , \tag{12}$$

where q is the z component of the field gradient tensor, and Q is the nuclear electric quadrupole moment.

3. Examples

A. $ACuX_3$

(i) $CsCuCl_3$

Schlueter[2] *et al.* have provided a refinement of a structure originally solved by Wells. The pertinent crystallographic parameters are displayed in Table I. The most important of these are the intra- and interchain Cu–Cu distances of 3.0621(10) Å and 7.2157(5) Å. The intrachain Cu–Cu distance is rather short but calculations of overlap integrals suggest that the metal-metal interaction is minimal.[2] This appears to be born out by magnetic measurements,[25–27] Table II. The magnetic behavior suggests that [1] effects dominate down to 30° K. At lower temperatures [3] coupling becomes more and more important until 10° K [3] ordering occurs. The onset of [3] ordering has also been observed by heat capacity measurements.[25]

DeJongh and Miedema[30] have interpreted the magnetic data as indicating that the interaction along the chain is ferromagnetic (in agreement with the ideas of Kanomori[44]) while the interchain interaction is antiferromagnetic.

Achiwa[26] found no ESR signal between 1.5° and 297° K for the concentrated crystal, presumably due to anisotropic exchange interactions. With Cu^{2+} as a 2% impurity in $CsMgCl_3$ a single line 1350G wide at g = 2.16 is observed. Neither angular nor temperature dependence have been reported.

From the ^{35}Cl NMR spectrum Rinneberg, *et al.*[62] found evidence for two different types of Cl bridges in $CsCuCl_3$.

This is consistent with the x-ray crystallographic results[2]. The covalency parameters indicate that the superexchange path involves predominately ligand p-orbitals, and very little sp-hybridization is present.

	A_s ($10^{-4}cm^{-1}$)	$A_{\sigma-\pi}$ ($10^{-4}cm^{-1}$)	f_s(%)	$f_{\sigma-\pi}$(%)	f_Q(%)
Cl_{gen}	9.1	6.1	0.61	11.9	20.3
Cl_{spec}	8.5	416	0.57	9.0	19.3

For the equally-bonded Cl_{spec} the z-axis of the electric-field gradient tensor was found to lie perpendicular to the Cu–Cl–Cu plane (parallel to [100]). For Cl_{gen} with only one strongly bonded Cu the z-axis of the EFG tensor lies along the Cu–Cl bond.

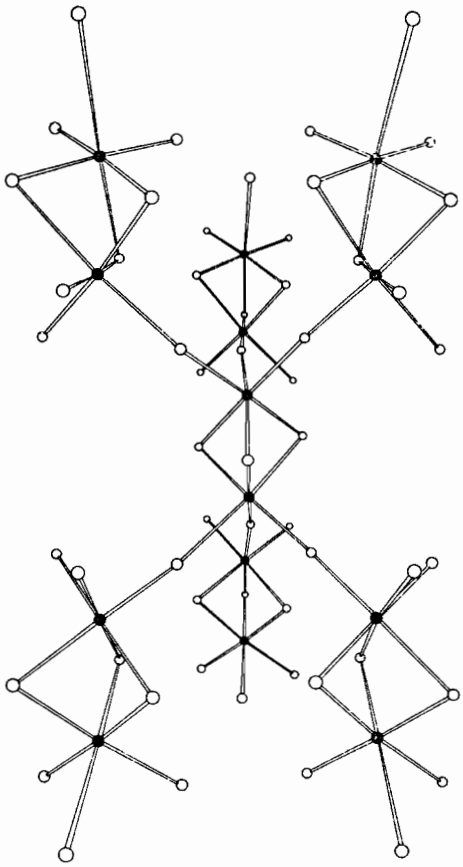

Figure 10. $CsCuBr_3$ structure. Adopted from Ref. 3.

Day[63] has recorded the visible absorption spectrum of this compound. It is not surprising that this spectrum is fairly uninteresting (two maxima: 11800 and 11000 cm^{-1}) as there is no possibility for d–d spin forbidden transitions in a d^9 system.

(ii) $CsCuBr_3$

The structure of this compound[3] is shown in Figure 10. While not an infinite chain it does possess chain-like qualities. Unlike the majority of compounds which will be discussed, this is a system in which strong magnetic coupling exists even at room temperature (μeff~ 0.11 B.M.) This is most likely due to a dominant 180° super exchange mechanism.

(iii) $(CH_3)_4NCuCl_3$

No data has been reported on this compound even though it is possible to prepare it as small hexagonal needles[20]. It would appear that its structure is similar

to that of $(CH_3)_4NMnCl_3$(TMMC) as it forms solid solutions with TMMC throughout an extensive range of concentrations. Tetramethylammonium trichlorocuprate (II) is a compound which should bear investigation as it may provide an opportunity to obtain a good example of an $S = {}^1/_2$ linear chain ferromagnet.

B. $ANiX_3$

(i) $(CH_3)_4NNiCl_3$

Due to the large interchain separation, 9.019 Å[4], one would expect a very good approximation to [1] behavior and, if Kanamori's ideas are to have any validity, an interaction of a ferromagnetic nature. One dimensional ferromagnetic behavior had indeed been observed. Gerstein, *et al.*[28] have investigated the powder susceptibility of $(CH_3)_4NNiCl_3$ between 1.6–79° K. Fisher's[64] infinite spin model provides the best fit ot the magnetic data in this temperature range. Interchain interactions indeed appear to be negligible as no [3] ordering was observed to 1.6° K. Unfortunately there have been no thermal or neutron diffraction measurements on this compound. The most probable reason for this deficiency is the difficulty of growing crystals of adequate size to allow single crystal measurements to be made.

Optical measurements on small crystals of $(CH_3)_4NNiCl_3$ have been performed at 5.80 and 300° K. As would be expected in a ferromagnetic system there is no evidence of exciton/magnon interaction. There does appear to be, however, a double exciton transition, ${}^3A_{2g} \rightarrow {}^3T_{2g} + {}^1E_g$, at ~ 19600 cm^{-1}. It would be worthwhile for a careful study to be made of the intensity vs. temperature for this band in order to compose the experimental variation with the predictions of Section 3.

(ii) $(CH_3)_4NNiBr_3$

Stucky *et al.*[5] have determined the structure of this compound. It belongs to space group $P6_3$ and is structurally the same as $(CH_3)_4NNiCl_3$[4].

There have been no magnetic investigations of this compound; therefore, we do not know whether it is also ferromagnetic. While the interchain separation is larger in the bromide than in the chloride, favoring ferromagnetic exchange[44], the 4p orbitals of the bromine atoms are more extensive than those of chlorine atoms favoring overlap and antiferromagnetic exchange. Stucki, *et al.*[5] have measured the absorption spectrum of a polycrystalline sample of $(CH_3)_4NNiBr_3$ at room temperature. The spectrum they report is routine for Ni^{2+} but bears repeating at lower temperatures.

(iii) N-$C_3H_7NH_3NiCl_3$, $C_5H_5NHNiCl_3$, and $C_5H_5NHNiBr_3$

Asmussen and Soling[29] have measured the magnetic susceptibilities of these three compounds between 100 and 300° K. All display moderately large, negative Weiss constants. To the present time there has been no structural work which would indicate that these compounds are indeed of the linear chain type; however, based upon their stoichiometry, Weiss constants and a typical coloration (red–brown) they would appear to be good candidates for investigation. These compounds are particularly important in that they may well display an interchain separation intermediate between the $(CH_3)_4N^+$ and the Cs^+ compounds and therefore intermediate magnetic properties.

(iv) $CsNiCl_3$

Achiwa[26] has measured both the single crystal magnetic susceptibility and electron spin resonance spectrum of $CsNiCl_3$. Using an isotropic $S = 1$ Heisenberg model scaled to the $S = 1$ Ising model he arrives at values of J of −11.0 and −12.1 (from T_m and χ_m respectively). This result differs somewhat from the result of $J = -14.2$ obtained from the powder magnetic susceptibility measurements of Smith *et al.*[31].

The ESR measurements of Achiwa show a single exchange narrowed line 1320G wide when $H_o \| c$ and 1190G wide with $H_o \perp c$. The line width decreases with decreasing temperature to about 25° K. ($\Delta H_{//} = 303G$, $\Delta H_\perp = 204G$). Below 25° K it broadens until it finally disappears at 4.5° K. There is a slight temperature dependence in the g-factor between R.T. and 77° K. Below 77° K the g-factor is constant. (297° K $g_{//} = 2.23_6$, $g_\perp = 2.24$; 77° K $g_{//}$ 2.24, $g_\perp = 2.24$).

Measurements of a dilute sample (~ 1%) of Ni^{2+} in $CsMgCl_3$[66] show a $g_{//} = 2.257$ and $g_\perp = 2.241$ at 77° K.

Minkiewicz, *et al.*[67] performed the original neutron diffraction measurements on $CsNiCl_3$. These results, obtained on a powder at 2° K suggested a transition at 4.5° K to an antiferromagnetic state in which the moments form a triangular array. The moment at 0° K was extrapolated to be $1.5\,\mu_B$ as opposed to the expected moment of about $2\,\mu_B$.

In contradiction to the above the ^{133}Cs NMR measurements of Clark and Moulton[68] suggested a collinear structure with magnetic transitions at 4.85 and 4.4° K. The parallel component of the internal hyperfine field, $H_{//}^{int}$, was estimated to be about 600G at 0° K: $H_\perp^{int} \rightarrow 0$ and the perpendicular components of the Ni^{2+} spin moments order.

Two recent neutron diffraction studies[69,70] support the triangular arrangement of Ni^{2+} moments (Figure 11) and provide a $\mu = 1.05$ at 0° K. Yelon and Cox[70] have

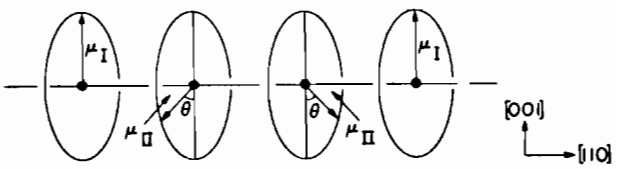

Figure 11. The Modified triangular model of Ni^{2+} moments in $CsNiCl_3$. Adopted from Ref. 70.

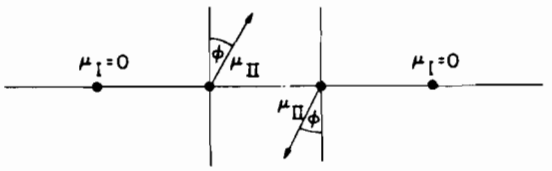

Figure 12. The collinear model of Ni^{2+} moments in $CsNiCl_3$. Adopted from Ref. 71.

suggested that the triangular model is consistent with all experimental data, including the NMR results. However, they also point out that the collinear model (Figure 12) gives precisely the same fit to the experimental data. There are, in fact, at least four models which account for the experimental results. Two are excluded on physical grounds. The triangular model is supported by similar results for $RbNiCl_3$[71], but Yelon and Cox conclude that the magnetic structures of materials of this type must depend on a delicate balance among anisotropy, crystal field effects, and weak basal-plane exchange.

Rinneberg, *et al.*[72] also observed the ^{35}Cl NMR for $CsNiCl_3$ and obtained results similar to those for Cl_{spec} (the equally-bridged Cl) in $CsCuCl_3$:

	A_s (10^{-4} cm^{-1})	$A_{\sigma\to\pi}$ (10^{-4} cm^{-1})	f_s(%)	$f_{\sigma\to\pi}$(%)	f_Q(%)
$CsNiCl_3$	4.3	1.9	0.58	7.3	15.1

The consistency in the covalency parameters in $CsNiCl_3$ and $CsCuCl_3$ is somewhat surprising considering the wide variation found in the KMF_3[73] compounds. This suggests that even at relatively high temperatures covalency is controlled more by collective interactions than by single ion effects. Clearly, however, much more evidence is required before this is definitely established.

The electronic spectra of $CsNiCl_3$ and Cs(Ni, Mg)Cl_3 have been measured to 80° K by McPherson and Stucky[74] and to 5° K by Ackerman, *et al.*[65]. All triplet→singlet transitions are anomolously intense suggesting cooperative effects are important. In contrast to the expected temperature dependence, described earlier, major increases in intensity vs. temperature occur both considerably above and around T_N. A careful study of band intensity is necessary however before much can be said about these effects. In addition a magnon side band is observed at 12719 cm^{-1} and a double exciton transition is seen at 13500 cm^{-1}.

Room temperature, single crystal infrared and Raman spectra have been assigned by Chadwick, *et al.*[75]

(v) $CsNiBr_3$

Stucky, *et al.*[5] have determined the structure of $CsNiBr_3$ to be the same as the $CsNiCl_3$ structure while Asmussen and Soling[29] have found the magnetic moment to be 3.42 with $\Theta = 101°$. Detailed optical measurements have been conducted at 300[65,74], 80[65,74] and 5° K[65]. An exciton/magnon transition is observed at 11779 cm^{-1} in the polarization perpendicular to the chain axis. As with $CsNiCl_3$ all the triplet→singlet transitions have anomalously enhanced intensities and a double exciton transition is seen (at 13500 cm^{-1}).

(vi) $CsNiI_3$

McPherson and Chang[7] have shown that $CsNiI_3$ belongs to spacc group $P6_3/mmc$ and is isomorphous with $CsNiCl_3$. They have also reported the low frequency (40–300 cm^{-1}) infrared absorption spectrum of this compound as well as a number of other compounds of ABX_3 formulation. McPherson[76] has measured the electrical conductivity of $CsNiI_3$ and finds it to be an ionic semiconductor exhibiting [3] conductivity.

No measurements of the electronic spectrum of $CsNiI_3$ have been reported.

(vii) $RbNiCl_3$

As with $CsNiCl_3$ there has been considerable controversy over the nature of the spin array in $RbNiCl_3$.

Asmussen and Soling[29] were the first to investigate $RbNiCl_3$ in any detail. They reported a moment of 3.47 μ_B and a Weiss constant of −112°. A later crystallographic investigation[8] demonstrated that the compound possessed the linear chain structure. A subsequent neutron diffraction study[67] indicted a Néel temperature of 11° K and suggested a spin arrangement similar to that found for $CsNiCl_3$. This latter conclusion was questioned by Epstein *et al.*[77] who suggested a collinear magnetic structure. Neutron diffraction studies on single crystals of $RbNiCl_3$[71] support the suggestion of a triangular array of spins but suggest that a slight modification to account for a small c-axis anisotropy is in order. The Néel temperature was found to be 11.15 ± 0.05° K.

The electronic spectrum of $RbNiCl_3$ shows the same basic features that $CsNiCl_3$ and $CsNiBr_3$ do[65,74]. One feature of note, however, is the appearance of the double exciton transition, $2(^3A_{2g}\to{}^3T_{2g})$ at 80° K but not at 300° K or at 4° K.[65] Such a temperature dependence suggests that long correlation lengths may be detrimental to the process.

Chadwick, *et al.*[75] have observed the single crystal infrared and Raman spectra. The transitions and assignments are similar to those for $CsNiCl_3$.

(viii) $RbNiBr_3$

Asmussen[8,29] has investigated both the magnetic and structural properties of this compound. These results are given in Tables I and II.

(ix) $CH_3NH_3NiCl_3$ and $TlNiCl_3$

Willett[9] has investigated both the structure and the room temperature spectrum of polycrystalline CH_3NH_3 $NiCl_3$. Although the space group to which this compound

belongs is Cmcm it possesses linear chains of face sharing octahedra. Because of the nature of the spectral measurements it is not possible to determine whether the electronic structure of $CH_3NH_3NiCl_3$ is modified by cooperative interaction.

$TlNiCl_3$, on the other hand displays the 'normal' $P6_3/mmc$ space group[10]. As the interchain separations in these two compounds, Table I, are the smallest of the $ANiX_3$ series an investigation of both the optical and magnetic properties of these compounds is in order.

C. $ACoX_3$

(i) $CsCoCl_3$

Soling[11] has determined the crystal structure of this compound and found it to be isostructural with $CsNiCl_3$ [space group $P6_3/mmc$, a = 7.2019(4) and c = 6.0315 (5) Å.]

For temperatures between 80° K and 300° K the magnetic susceptibility was far below the expected spin only value.[11] Further magnetic investigations were made by Achiwa,[26] who has shown that antiferromagnetism in $CsCoCl_3$ arises from the contributions of the symmetry split $^4T_1(^4F)$ ground state. This state is split by the spin-orbit coupling and the trigonal crystal field into three Kramers doublets so that an effective $S' = {}^1/_2$ is appropriate. The results are $J_{//} = -85°$ K and an estimated value for $J_\perp$ of between 10 and 17° K. These values indicate that $CsCoCl_3$ approximates a [1] system above about 10° K.

The EPR spectrum of a pure concentrated crystal of $CsCoCl_3$ does not seem to have been measured; however, 1% Co^{+2} in $CsMgCl_3$ has been studied by Achiwa[26] who found $g_{//} = 7.32$ and $A(Co^{2+}) = 330 = 10^{-4}$ cm^{-1}. This is in agreement with $g_{//} = 7.4$ found from susceptibility measurements. Rinneberg and Hartmann[72] also measured the dilute Co^{+2} EPR with following results:

	$g_{//}$	$g_\perp$	$A_{//}(Co^{2+})$	$A_\perp(Co^{2+})$
R and H	7.37	2.51	330×10^{-4} cm^{-1}	
Achiwa	7.40	4.3	339×10^{-4} cm^{-1}	21×10^{-4} cm^{-1}

The ^{35}Cl NMR has been analyzed[72] with the following results:

	A_s (10^{-4} cm^{-1})	$A_{\sigma-\pi}$ (10^{-4} cm^{-1})	f_s(%)	$f_{\sigma-\pi}$(%)	f_Q(%)
$CsCoCl_3$	2.68	1.03	0.54	6.0	8.4

Comparison of these results with those for $CsCuCl_3$ and $CsNiCl_3$ indicate that the covalency in the M–Cl–M bonds in these compounds is remarkably similar.

Rinnebert and Hartmann[72] have observed the optical spectrum at 80° K which is essentially the same as the room temperature spectrum, and have obtained the following parameter values: Dq = 600 cm^{-1} and E_p = E(4p)–E(4_F) = 12.000 cm^{-1}. No trigonal splitting was observed. Gilmore[78] observed the 4.2° K spectrum of polycrystalline films of $CsCoCl_3$ and obtained similar results: Dq = 685 cm^{-1}, B = 740 cm^{-1}. However, he did find anomalous intensities in ten doublet bands which he attributed to exchange interactions. The present authors have reexamined the polarized optical spectra of single crystals of $CsCoCl_3$ at 4° K and above, and have observed temperature dependent bands which do not correlate with the known phonon modes[7,75] and may be attributed to exciton-magnon interactions.

(ii) $RbCoCl_3$

Engberg and Soling[12] originally prepared and structurally characterized $RbCoCl_3$ as being isomorphous with $CsNiCl_3$ with a = 6.89 Å and c = 5.99 Å Gilmore[78] later observed the polycrystalline optical spectrum at 4.2° K and assigned the following parameter values in terms of O_h symmetry: Dq = 740 cm^{-1}, B = 780 cm^{-1}.

(iii) $TlCoCl_3$

$TlCoCl_3$ was prepared and examined *via* x-ray powder photography by Zodkevetz, *et al.*[10] who have shown to be isomorphic with $CsNiCl_3$ and a = 6.90 A, c = 5.98 Å.

D. $AFeX_3$

(i) $RbFeCl_3$

This compound presents a somewhat confusing picture. It has been investigated by several workers who have interpreted their results in a conflicting manner. Achiwa[26] analyzed the magnetic susceptibility data in terms of the molecular field model of Moriya[51] assuming a fictitious spin S' = 1 for the orbital triplet arising from the ^5D configuration. For temperatures below 105° K the calculation results in an antiferromagnetic interaction with $J_{//} = -11.5°$ K and $J_\perp = -3.8°$ K. Above ~105° K Achiwa finds appreciable contributions from the excited orbital doublet. According to his interpretation the direct exchange interaction, e_g–e_g', which was found to be small and apparently positive, compensates the large, negative (–15° K) superexchange path, t_2–pσ–t_2, where pσ is an sp^2 hybrid of chlorine orbitals.

Witteveen and vanVeen[33] reexamined $RbFeCl_3$ and state that their results are in agreement with those of Achiwa:[26] in the low temperature region (<80° K) $\mu_{eff} = -5.95\,\mu_B$, $J_{//} = -6 \pm 2°$ K and $J_\perp = -1.6 \pm 2°$ K. Unfortunately they report Achiwa's values incorrectly. The correct values are $\mu_{//} = 6.70\,\mu_B$, $\mu_\perp = 6.35\,\mu_B$, $J_{//} = -11.5°$ K, $J_\perp = -3.8°$ K. Witteveen and vanVeen[33] extracted the parallel and perpendicular exchange constants from χ calculated according to Moriya's[51] molecular field theory as in Achiwa's work.

Montano, *et al.*[79] have measured the temperature dependence of the electric field gradient (from Mössbauer measurements) in the range 4.2–300° K (T_N = 2.55° K). Their Hamiltonian describing the system

contained a single-ion crystal field term and an anisotropic bilinear interaction between nearest-neighbor Fe^{2+} ions. Assuming a ferromagnetic interaction with the Fe^{2+} spins lying in the basal plane they were able to obtain a good fit of Achiwa's[26] susceptibility data with $J_{//} = 7.2°$ K and $J_{\perp} = 15.8°$ K.

Below T_N Montano, *et al.* use a one-dimensional spin-wave theory similar to that used to treat $RbNiCl_3$ and $CsNiCl_3$.[60] Their value for the magnetic moment per Fe^{2+} ion at 0° K is 2.2 μ_B in agreement with the neutron scattering results of Davidson, *et al.*[80] but considerably reduced from $\mu_{//} = 6.7\,\mu_B$, $\mu_{\perp} = 6.35\,\mu_B$ determined from Achiwa's susceptibility measurements. These results are significant in that they imply that [1] effects predominate even below the [3] ordering temperature.

As pointed out by deJongh and Miedema[30] $RbFeCl_3$ is a clear example of the problems associated with deducing magnetic structure from susceptibility measurements alone.

The i.r. and Raman spectra[75] are generally similar to the $CsNiCl_3$ spectra except that several modes are either absent or of very low intensity.

(ii) $TlFeCl_3$, NH_4FeCl_3 and $CsFeCl_3$

The susceptibilites and x-ray structures of these compounds have been reported by Witteveen and vanVeen[33]. The results are listed in Tables I and II.

Clearly much work remains to be done before the $AFeCl_3$ system is well-understood. Apparantly neither optical nor EPR data are available. Although the $3d^6$ configuration is usually difficult to interpret, these data should help clarify some of the confusion surrounding these compounds.

E. $AMnX_3$

(i) $(CH_3)_4NMnCl_3$

Tetramethylammonium trichloromanganate (II) (TMMC) is the best example of a truly [1] linear chain antiferromagnet in the ABX_3 series. As a result it has been one of the more extensively studied compounds of the series.

At room temperature TMMC has been reported by Morosin and Graeber[15] to belong to the hexagonal space group $P6_3/m$ with a_o (interchain separation) = 9.1510 Å, c_o = 6.4940 Å, and a Mn-Mn distance of 3.25 Å. (Occasionally a monoclinic form has been observed). At 128° K there is evidence from x-ray, Raman and neutron diffraction studies for a hexagonal → monoclinic phase change. Additional neutron-diffraction peaks below 128° K were found to be consistent with a monoclinic structure involving a repacking of the $MnCl_3$ units with no change in [1] character of the magnetic properties[81]. The x-ray data is also consistent with a monoclinic structure in which a_o almost doubles (a_o = 15.488, b_o = 6.459, c_o = 9.038 Å with the preferred space group ($P2_2/m$).[16]

From the x-ray data it was concluded that the tetramethylammonium (TM) groups are ordered below ~128° K. A similar conclusion was inferred by comparison between the Raman scattering spectra at 298° K and 10° K.[16] However, no spectra were reported for the region around 128° K.

That the TM groups order at 120° K has been disputed by Mangum and Utton[81] who have examined the proton magnetic resonance (PMR) of the TM protons in the region 0.4–300° K. Between 6° and 39° K comparison of the PMR spectra taken with the static magnetic field parallel with the c axis (H//c) and spectra taken when $H_{\perp}$ c demonstrates that in this region the TM groups are stationary. Between 36° and 50° K a good fit of the observed spectrum is obtained by assuming the protons begin to rotate in a plane normal to the N–C axis. Above 50° K the spectrum consists of a single unstructured broad line independent of both temperature and orientation.

A careful x-ray study of the room temperature monoclinic form of TMMC could help resolve this problem.

Magnetic susceptibilities of TMMC have been reported by Dingle, *et al.*[24] from room temperature to below 1° K. Interpreting the data in terms the Bonner and Fisher model[43] scaled to $S = {}^5/_2$ they obtain J = –6.3° K for the intrachain exchange constant and estimated the interchain interaction to be several orders of magnitude smaller.

A somewhat higher value of J = –7.7° K was found by Birgeneau, *et al.*[83] using quasielastic neutron scattering. They found TMMC to be fully [1] down to 1.1° K and could quantitatively fit their data at all temperatures with Fisher's[64] model for a classical Heisenberg chain.

Hutchings, [81] *et al.* have carefully analyzed the time-dependent magnetic correlations in deuterated TMMC and arrived at J = –6.6° K. This value compared favorably with J = –6.47° K found from the analysis of the static susceptibility in terms of Rushbrooke and Wood's[84] quantum mechanical series expansion.

Dingle, *et al.*[24] tentatively assigned $T_N = 0.84°$ K for the transition to [3] order, but, due to probable impurity complications were unable to confirm this. Mangum and Utton[82] observed the PMR spectrum of the TM ions with $H_o \perp$ c and found no evidence for a cooperative transition below 1° K. On reexamining the PMR spectrum with H_o c Dupas and Renard[85] observed an abrupt change at 0.85° K which they interpret as a transition to long range [3] order.

Assuming T_N is indeed 0.84 ± 0.01° K the required intra- and interchain couplings are estimated[24,85] to be J = –6.5° K and -10^{-3} respectively.

A central feature in the study of TMMC and indeed in all [1] compounds is the elucidation of the formation of short range spin-correlations without a definite transition to long range order. Dietz, *et al.*[86] have studied the Mn^{2+} ESR spectrum and found it to differ sharply from the predictions of [3] exchange-narrowing

theory. They could, however, account for the anomalies by assuming a long-time persistence of [1] spin-correlations. These results together with those of Hutchings, *et al.*[81] suggest that [1] spin-wave theory is indeed applicable to TMMC, particularly at low temperatures.

The existence of spin-waves should give rise to magnon sidebands in the optical spectrum. Although anomalous bands and intensities are observed[24,87] in the TMMC spectra, the role of exchange coupling is uncertain at the present time. In view of recent assignment of the Raman and far-infrared phonon spectra of TMMC[88] a reexamination of the optical spectrum could be helpful.

(ii) $CsMnCl_3$

This compound is unique among the ABX_3 series in its rhombohedral structure (space group $R\bar{3}m$). A hexagonal unit cell (a = 7.288 Å, c = 27.44 Å) with nine formula units has been proposed.[17] Other investigations[36,89] have confirmed and refined this structure. The unit cell consists of three $Mn_3Cl_{12}^{6-}$ units arranged in a stairstep-like array with three $MnCl_6^{4-}$ octahedra sharing faces then a single linear bridge (shared corner) to the next $Mn_3Cl_{12}^{6-}$ unit.

A single paramagnetic line has been observed by Kedzie, *et al.*[35] to broaden from 40G at 297° K to 240G at 77° K and then disappear asymptotically near 70° K. Below 70° K an antiferromagnetic resonance (AFMR) appears. Approaching the transition temperature from both sides they find $T_N = 69° \pm 3°$ K. From observations of the AFMR with $H_{o\perp}c$ Kedzie, *et al.*[90] conclude that the sublattice magnetization directions are normal to the $\underset{\sim}{c}$ axis.

Rinneberg and Hartmann[72] have interpreted the ^{35}Cl NMR spectrum to obtain the shf constants and covalency parameters:

	A_x (10^{-4} cm^{-1})	$A_{\sigma-\pi}$ (10^{-4} cm^{-1})	f_s(%)	$f_{\sigma-\pi}$(%)	f_Q(%)
Cl_{II} (linear bridge)	1.70	0.0	0.57	0	8.2
Cl_I (bent bridge)	1.46	0.06	0.50	0.6	7.4

Comparison with previous results for $CsBCl_3$ (B = Cu^{2+}, Ni^{2+}, Co^{2+}) indicates a trend of decreasing covalency in the metal–chlorine bond when going from copper to magnanese. These same authors also looked at the pure NQR frequencies for the two chlorine positions at 77° K and at ~20° K and found no evidence for a transition to the ordered state above 20° K. A transition temperature of (67 ± 2)° K has, however, been confirmed by neutron diffraction.[36]

The neutron diffraction results have led Melamud, *et al.*[36] to propose an antiferromagnetic structure consisting of alternating ferromagnetic planes stacked along the $\underset{\sim}{c}$ axis in which neighboring planes have antiparallel spins. The magnetic structure exhibits monoclinic symmetry similar to many perovskites.

The fluorescence spectra of $CsMnCl_3$ shows only a slight (10%) increase in intensity from 25° K to 70° K followed by a gradual decrease between 70° K and 240° K.[1,2]

The single crystal ESR of Mn^{2+} in $CsMgCl_3$ (space group $P6_3/mmc$) has been reported.[66] As expected for $I = {}^5/_2$, $S = {}^5/_2$ it consists of a six line hyperfine spectrum superimposed on each line of a five line fine structure spectrum. The results are $\underset{\sim}{g}_{//} = 2.0016$, $\underset{\sim}{g} = 2.0015$, $\underset{\sim}{D}$ (gauss) = 313, $\underset{\sim}{A}$ (gauss) = 86.5.

(iii) $RbMnCl_3$

A hexagonal structures (space group $P6_3/mmc$) with six magnetic ions per unit cell has been proposed[17,36] for this compound. This structure is similar to but not isomorphus with the $CsNiCl_3$ structure.

Kedzie, *et al.* have observed the ESR spectra of $RbMnCl_3$ at low temperatures[35,90]. In the paramagnetic region $RbMnCl_3$ shows similar linewidth variation to $CsMnCl_3$. In the antiferromagnetic region up to eight narrow lines are found. The ordering temperature is found from the asymptotic broadening of the linewidths to be $T_N = (86 \pm 6°)$° K.

Melamud, *et al.*[36] have analyzed their neutron diffraction data on the basis of the magnetic and crystallographic unit cells being identical. They assign the magnetic structure as consisting of ferromagnetic planes stacked along the $\underset{\sim}{c}$-axis with alternating spin direction. The spin moments lie perpendicular to the c-axis. They also calculate a magnetic moment of 4.1 μ_B (at 4.2° K).

The fluorescence spectra of $RbMnCl_3$ show large changes in intensity above T_N, but relatively small changes below T_N.

(iv) $CsMnBr_3$

This compound has been reported to be isostructural with $CsNiCl_3$.[18] McPherson, *et al.*[93] have reported the optical spectrum to be generally similar to that of TMMC. However, they suggest that the intensities appear to be strongly affected by exchange interactions in contrast with the observations[24,87] for TMMC. These same authors also report a calculated value of $\mu_{eff} = 6.4\ \mu_B$.

Further work on this compound should yield interesting results since the possibility for direct exchange is reduced and enhanced for superexchange relative to $CsMnCl_3$.

F. $ACrX_3$

(i) $CsCrCl_3$

$CsCrCl_3$ is the only member of the $ACrX_3$ series which has received any serious attention. Seifert and Klatyk[21] prepared the compound and reported its structure as being of the $CsNiCl_3$ type.

This was followed by the work of Larkworthy and Trigg[41] who reported both the reflectance spectrum of $CsCrCl_3$ and that the compound is antiferromagnetic ($\mu_{eff} = 3.31\,\mu_B$ at 300° K, $1.95\,\mu_B$ at 90° K).

More recently McPherson, *et al*[20] have reported both the structure and single crystal polarized spectrum $CsCrCl_3$. The structure is similar to the $CsNiCl_3$ structure except that a small distortion from trigonal symmetry exists. The most important feature of the spectrum, measured at 80° K is the appearance of a double exciton band, $2(^5E \rightarrow {}^5T_2)$, at ~20000 cm^{-1}. As has already been noted for other members of the ABX_3 series the spin forbidden transitions are all anomalously intense.

Hardt and Streit[19] have prepared a series of $ACrCl_3$ compounds with A = Cs^+, Rb^+, $(CH_3)_4N^+$, NH_4^+, and PyH^+, and two $ACrBr_3$ compounds with A = Cs^+ and $(CH_3)_4N^+$. They report that all compounds except NH_4CrCl_3 apparently have a distorted hexagonal perovskite ($CsNiCl_3$) structure. The distortion is attributed to a Jahn–Teller mode.

G. AVX_3

(i) $(CH_3)_4NVCl_3$

Seifert, *et al.*[22] have determined $(CH_3)_4NVCl_3$ to belong to a hexagonal space group with cell constants, $\underset{\sim}{a} = 9.146$ Å and $\underset{\sim}{c} = 6.227$ Å for $z = 2$ suggesting that this compound may possess a linear chain structure. Magnetic measurements show a change in moment from $1.30\,\mu_B$ at 80° K to $2.13\,\mu_B$ at 289° K. Larkworthy, *et al.*[41] have repeated these measurements, obtaining essentially the same results, and suggest that the susceptibilities are suspect due to contamination by a hydrated species. These latter authors also report the diffuse reflectance spectrum of $(CH_3)_4NVCl_3$. While broad features are discernable, the spectrum is not of sufficient quality to provide useful information about cooperative effects.

(ii) $CsVCl_3$

Work on $CsVcl_3$ has been limited to the determination of the cell constants and the magnetic moment: $2.02\,\mu_B$ at 370° K and $0.98\,\mu_B$ at 82° K.

(iii) $RbVCl_3$

Grey and Smith[23] have reported that $RbVCl_3$ is isostructural with $CsNiCl_3$ and have recorded both the magnetic susceptibility and the electronic absorption spectrum of $RbVCl_3$. A magnetic moment of 1.85 B.M. at 300° K with a $J = -151$ is found for $RbVCl_3$. The electronic reflectance spectrum shows additional bands over what would be expected over a normal V^{2+} spectrum These are interpreted in terms of trigonal components of the $^4A_2 \rightarrow {}^4T_1$ spin allowed, transitions. It is unlikely that such is the case, the most plausible explanation relating to an intensity enhancement of spin forbidden bands due to cooperative effects. Indeed such an explanation has been suggested by Larkworthy.[41] Certainly the spectrum deserves reinvestigation at low temperatures.

(iv) $KVCl_3$

$KVCl_3$ is isomophous with $CsNiCl_3$[94] and has had its optical[95] but not its magnetic properties reported. The spin forbidden bands show anomolous intensity as might be expected and a portion of the spectrum has been assigned. There is however, with this compound as well as with the other AVX_3 compounds, a great deal of work yet to be done before the magnetic and optical properties of the AVX_3 series is elucidated.

4. References

1 For example see the summary by D.D. Sell, *J. Appl. Phys., 39,* 1030 (1968).
2 A.W. Schleuter, R.A. Jacobson and R.E. Rundle, *Inorg. Chem., 5,* 277 (1966).
3 T. Li and J.D. Stucky, *J. Chem. Phys.,* In press.
4 G.D. Stucky, *Acta Cryst., B24,* 330 (1968).
5 G.D. Stucky, S.D. Agostino, and J. McPherson, *J. Am. Chem. Soc., 88,* 4828 (1966).
6 G.N. Tischemko, Tn. Inst. Kristallogr., *Akad. Nauk SSR, 11,* 93 (1955).
7 J. McPherson, and J.R. Chang, *Inorg. Chem., 12,* 1196 (1973).
8 R.W. Asmussen, T. Kindt Larsen and H. Soling, *Acta Chem. Scand., 23,* 2055 (1969).
9 R.D. Willett, *J. Chem. Phys., 45,* 3737 (1966).
10 A. Zodkevitz, J. Makovsky and Z.H. Kalman, *Israel J. Chem., 8,* 755 (1970).
11 H. Soling, *Acta Chem. Scand., 22,* 2793 (1968).
12 A. Engberg and H. Soling, *Acta Chem. Scand., 21,* 168 (1967).
13 M. Amit, A. Zodkevitz, and J. Makovsky, *Israel J. Chem., 8,* 737 (1970).
14 H.J. Seifert and K. Klatyk, *Z. anorg. u. allgem. Chem., 342,* 1 (1966).
15 B. Morosin and E.J. Graeber, *Acta Cryst., 23,* 766 (1967).
16 P.S. Purcy and B. Morosin, *Phys. Lett., 36A,* 409 (1971).
17 T.I. Li, G.D. Stucky, and G.L. McPherson, *Acta Cryst., B29,* 330 (1973).
18 J. Goodyear and D.J. Kennedy, *Acta Cryst., B28,* 1640 (1972).
19 H.D. Hardt and G. Streit, *Z. allgem. u. anorg. Chem., 373,* 97 (1970).
20 G.L. McPherson, T.J. Kistenmacher; J.B. Folkers and G.D. Stucky, *J. Chem. Phys., 57,* 3771 (1972).
21 H.J. Seifert and K. Klatyk, *Z. anorg. u. allgem. Chem., 334.* 113 (1964).
22 H.J. Seifert and P. Ehrlich, *Z. anorg. u. allgem. Chem., 302,* 284 (1959).
23 I.E. Grey and P.W. Smith, *Chem. Comm.,* 1525 (1968).
24 R. Dingle, M.E. Lines, S.L. Holt, *Phys. Rev., 187,* 643 (1969).
25 F.J. Rioux and B.C. Gerstein, *J. Chem. Phys., 50,* 758 (1969).
26 N. Achiwa, *J. Phys. Soc. Japan, 27,* 561 (1969).
27 *F.J. Rioux and B.C. Gerstein, J. Chem. Phys., 53,* 1789 (1970).
28 B.C. Gerstein, F.D. Gehring and R.D. Willett, *J. Appl. Phys., 43,* 1932 (1972).

29 R.W. Asmussen and H. Soling, *Z. anorg. u. allgem. Chem., 283,* 1 (1956).
30 L.J. de Jongh and A.R. Miedema, *Adv. in Phys.,* In press.
31 J. Smith, B.C. Gerstein, S.H. Liu, and G. Stucky, *J. Chem. Phys., 53,* 418 (1970).
32 H. Soling, *Acta Chem. Scand., 22,* 2793 (1968).
33 H.T. Witteveen and J.A.R. van Veen, *J. Chem. Phys., 58,* 186 (1973).
34 R.W. Asmussen, as reported in Ref. 36.
35 R.W. Kedzie, J.R. Shane, M. Kestigian, and W.J. Croft, *J. Appl. Phys., 36,* 1195 (1965).
36 M. Melamud, J. Makovsky, and H. Shaked, *Phys. Rev., B3,* 3873 (1971).
37 J.R. Shane, R.W. Kedzie, and M. Kestigian, *J. Appl. Phys., 37,* 1134 (1966).
38 M. Melamud, J. Makovsky, and Shaked, *Phys. Rev., B3,* 821 (1971).
39 M. Melamud, H. Pinto, G. Shachar, J. Makovsky, and H. Shaked, *Phys. Rev., B3,* 2344 (1971).
40 D.J.W. Tjdo as reported in Ref. 41.
41 L.F. Larkworthy and J.K. Trigg, *Chem. Comm.,* 1221 (1970).
42 H.J. Seifert, H. Fink, and E. Just, *Naturwiss., 6,* 297 (1968).
43 J.C. Bonner and M.E. Fisher, *Phys. Rev.,* 135, A640 (1964).
44 J. Kanamori, *J. Phys. Chem. Sol., 10,* 87 (1959).
45 P.W. Anderson, *Phys. Rev., 79,* 350 (1950).
46 J.C. Slater, *Quart. Progr. Rept. M.I.T.,* July 15, 1; Oct. 15,1 (1953).
47 J.B. Goodenough, *Phys. Rev., 100,* 564 (1955).
48 J. Yamashito and J. Kondo, *Phys. Rev., 109,* 730 (1958).
49 D.L. Dexter and R.S. Knox, *Excitons,* Interscience, New York, 1965.
50 An excellent treatment of exciton theory as applied to ionic crystals is given by R. Loudon, *Adv. Phys., 17,* 243 (1968).
51 T. Moriya, *J. Phys. Soc. Japan, 21,* 926 (1966).
52 F.D. Sell, R.L. Greene and R.M. White, *Phys. Rev., 158,* 489 (1967).
53 R.E. Dietz and A. Misetich, in *Proceedings of the conference on Localized Excitations in Solids,* Irvine, California, 1967 (Plenum, New York, 1968), p. 366.
54 S.E. Stokowski and D.D. Sell, *Phys. Rev., B3,* 208 (1971).
55 K. Motizuki and L. Harado, *Solid State Commun., 8,* 951 (1970).
56 H. Tanaka, *J. Phys. Soc. Japan, 31,* 368 (1971).
57 K. Shinagawa and Y. Tanabe, *J. Phys. Soc. Japan, 30,* 1280 (1971).
58 T. Fujiwara and Y. Tanabe, *J. Phys. Soc. Japan, 32,* 912 (1972).
59 T. Fujiwara, W. Gebhardt, K. Pentanides, and Y. Tanabe, *J. Phys. Soc. Japan, 33,* 39 (1972).
60 See for example, P.A. Montano, E. Colun, and H. Shechter, *Phys. Rev., B6,* 1053 (1972).
61 R. Bersohn and R.G. Shulman, *J. Chem. Phys., 45,* 2298 (1966); F. Keffer, T. Oguchi, W. O'Sullivan, and J. Yamashita, *Phys. Rev., 115,* 1553 (1959).
62 H. Rinneberg, H. Haas, and H. Hartmann, *J. Chem. Phys., 50,* 3064 (1969).
63 P. Day, *Proc. Chem. Soc., 18,* (1964).
64 M.E. Fisher, *Am. J. Phys., 32,* 343 (1964).
65 J. Ackerman, E.M. Holt, and S.L. Holt, *J. Sol. State Chem.,* In press.
66 G.L. Mc Fherson, T.J. Kistenmacher and G.D. Stucky, *J. Chem. Phys., 52,* 815 (1970).
67 V.J. Minkiewicz, D.E. Cox, and G. Shirane, *Solid State Comm., 8,* 1001 (1970).
68 R.H. Clark and W.G. Moulton, *Phys. Rev., B5,* 788 (1972).
69 D.E. Cox and V.J. Minkiewicz, *Phys. Rev., B4,* 2209 (1971).
70 W.B. Yelon and D.E. Cox, *Phys. Rev., B7,* 2024 (1973).
71 W.B. Yelon and D.E. Cox, *Phys. Rev., B6,* 204 (1972).
72 H. Rinneberg and H. Hartmann, *J. Chem. Phys., 52,* 5814 (1970).
73 R.G. Schulman and K. Knox, *Phys. Rev. Lett., 4,* 603 (1960).
74 G.L. McPherson and G.D. Stucky, *J. Chem. Phys., 57,* 3780 (1972).
75 A. Chadwick, J.T.R. Dunsmuir, I.W. Borest, and A.P. Lane, *J. Chem. Soc. (A),* 2794 (1971).
76 G.L. McPherson, personal communication.
77 A. Epstein, J. Makovsky, and H. Shaked, *Sol. State Comm., 9,* 249 (1971).
78 F.C. Gillmore, U.S. Atomic Energy Commission, 1969 ORNL TM–2507.
79 P.A. Montano, E. Cohen, H. Shechter, and J. Makovsky, Phys. Rev., B7, 1180 (1973).
80 G.R. Davidson, M. Eibschutz, D.E. Cox, and V.J. Minkiewicz, in *Seventeen Conference on Magnetism and Magnetic Materials,* Chicago, 1971, edited by C.D. Graham and J.J. Rhyne (AIP, New York, 1972).
81 M.T. Hutchings, G. Shirane, R.J. Birgeneau, and S.L. Holt, *Phys. Rev., B5,* 1999 (1972).
82 B.W. Mangum and D.B. Utton, *Phys. Rev., B6,* 2799 (1973).
83 R.J. Birgeneau, R. Dingle, M.T. Hurchings, G. Shirane, and S.L. Holt, *Phys. Rev. Lett., 26,* 718 (1971).
84 G.S. Rushbrooke and P.J. Wood, *J. Mol. Phys., 1,* 257, (1958).
85 C. Dupas and J.P. Renard, *Phys. Lett., 43A,* 119 (1973).
86 R.E. Dietz, F.R. Merritt, R. Dingle, D. Horne, B.G. Silbernagel, and P.M. Richards, *Phys. Rev. Lett., 26,* 1186 (1971).
87 K.E. Lawson, *J. Chem. Phys., 47,* 3627 (1967).
88 D.M. Adams and R.R. Smardzewski, *Inorg. Chem., 10,* 1127 (1971).
89 T. Li, G.D. Stucky and G.L. McPherson, *Acta. Cryst.* (to be published).
90 R.W. Kedzie, J.R. Shane, and M. Kestigian, *Bull, Am. Phys. Soc., 10,* 315 (1965).
91 W.W. Holloway, Jr. and M. Kestigian, *Phys. Lett., 29A,* 709 (1969).
92 M. Kestigian and W.W. Holloway, Jr., *Phys. Stat. Sol., A6,* K19 (1971).
93 G.L. McPherson, H.S. Aldrich, and J.R. Chang, *Inorg. Chem.* (to be published).
94 H.J. Seifert and P. Ehrlich, *Z. anorg. u. allgem. Chem., 302,* 284 (1959).
95 W.E. Smith, *J. Chem. Soc. (A),* 2677 (1969).
96 C. Kittel, Introduction to Solid State Physics, 4th edition, Wiley, New York, 1971, p. 539.